International Journal of Pharmaceutics 493 (2015) 412–425

Contents lists available at ScienceDirect

International Journal of Pharmaceutics

journal homepage: www.elsevier.com/locate/ijpharm

Formulation and process factors influencing product quality and *in vitro* performance of ophthalmic ointments

Xiaoming Xu, Manar Al-Ghabeish, Ziyaur Rahman, Yellela S.R. Krishnaiah, Firat Yerlikaya, Yang Yang, Prashanth Manda, Robert L. Hunt, Mansoor A. Khan*

Food and Drug Administration, CDER/OPQ/OTR/DPQR, 10903 New Hampshire Avenue, Silver Spring, MD 20993, USA

ARTICLE INFO

Article history:
Received 29 May 2015
Received in revised form 20 July 2015
Accepted 26 July 2015
Available online 29 July 2015

Keywords:
Ophthalmic ointments
Acyclovir
In vitro release testing
Corneal drug permeation
Rheology
Yield stress
Equivalence evaluation
Multivariate analysis
Design of experiments (DoE)

ABSTRACT

Owing to its unique anatomical and physiological functions, ocular surface presents special challenges for both design and performance evaluation of the ophthalmic ointment drug products formulated with a variety of bases. The current investigation was carried out to understand and identify the appropriate *in vitro* methods suitable for quality and performance evaluation of ophthalmic ointment, and to study the effect of formulation and process variables on its critical quality attributes (CQA). The evaluated critical formulation variables include API initial size, drug percentage, and mineral oil percentage while the critical process parameters include mixing rate, temperature, time and cooling rate. The investigated quality and performance attributes include drug assay, content uniformity, API particle size in ointment, rheological characteristics, *in vitro* drug release and *in vitro* transcorneal drug permeation. Using design of experiments (DoE) as well as a novel principle component analysis approach, five of the quality and performance attributes (API particle size, storage modulus of ointment, high shear viscosity of ointment, *in vitro* drug release constant and *in vitro* transcorneal drug permeation rate constant) were found to be highly influenced by the formulation, in particular the strength of API, and to a lesser degree by processing variables. Correlating the ocular physiology with the physicochemical characteristics of acyclovir ophthalmic ointment suggested that *in vitro* quality metrics could be a valuable predictor of its *in vivo* performance.

Published by Elsevier B.V.

1. Introduction

Ocular delivery of pharmaceuticals in ointment bases is fairly common among all approved drug products in the US, and it accounts for approximately 10% of the products, trailing only to eye drop solutions (drugs@FDA) (Fig. 1). Clinically, ophthalmic ointments serve as a viable dosage form for localized treatment of eye diseases, such as glaucoma, infections and inflammatory conditions. (Høvding, 1989; Robin and Ellis, 1978; Wilhelmus et al., 1993)

Ocular surface presents unique challenges for both formulation design and performance evaluation of ophthalmic drug products: (1) it constitutes the outermost region of the eye, the organ responsible for vision, and fulfills three most vital functions, *i.e.*, optical (to transmit light), mechanical (blinks more than 14 thousand times per day to moisten for lubrication and to eliminate foreign objects), and immunological (to provide defense against bacterial and viral infections) (Doane, 1980; Katami, 1991; Le Discorde et al., 2003; VanderWerf et al., 2003); hence any topically applied drug product should withstand the high shear of the blinking to prevent pre-corneal clearance (Gaudana et al., 2010) in order to achieve its therapeutic effect, and doing so without interference with the normal function of the eye; (2) the site-of-action for most ophthalmic drug products is restricted primarily to the ocular surface and/or interior eye tissues, and hence the clinical performance assessment of the topically applied ophthalmic drug products including ointments is dependent on the interplay of the physicochemical factors governing the drug release and physiological environment of the complex ocular surface responsible for drug absorption. These challenges not only limit the development of more effective drug products for ophthalmic use, but also increase regulatory hurdles for drug approval, particularly for generic ophthalmic drug products.

Abbreviations: BE, bioequivalence; CMA, critical material attributes; CPP, critical process parameters; CQA, critical quality attributes; DoE, design of experiments; HSV, herpes simplex virus; ICH, international conference on harmonisation; IVRT, *in vitro* release testing; PCA, principle component analysis; RLD, reference listed drug; USP, United States pharmacopeia; VZV, varicella-zoster virus.

* Corresponding author. Fax: +1 301 796 9816.
E-mail address: Mansoor.Khan@fda.hhs.gov (M.A. Khan).

http://dx.doi.org/10.1016/j.ijpharm.2015.07.066
0378-5173/Published by Elsevier B.V.

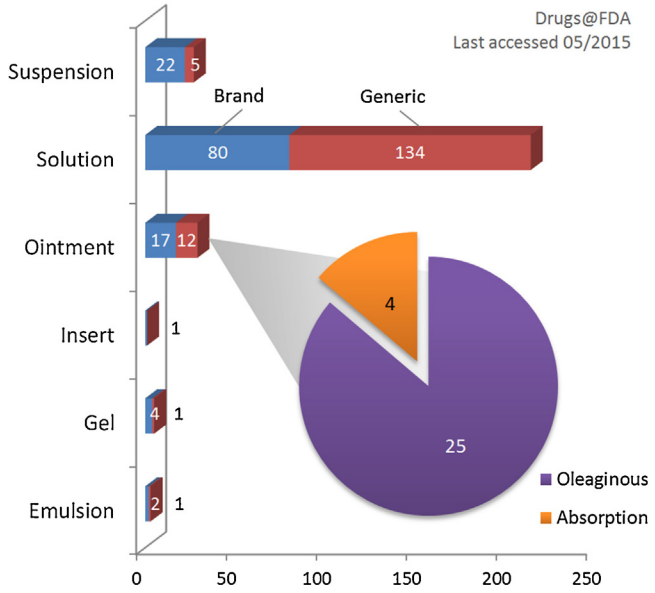

Fig. 1. Various types of dosage forms approved for ophthalmic use in the US.

The availability of product quality metrics is critical to demonstrate that generic pharmaceutical drug products are therapeutically equivalent and interchangeable with their associated innovator's product. Sameness evaluations are also needed when a firm decides to change excipients, processes, sites, *etc.* or in some cases when a variant of the original dosage form is changed to a new dosage form. A list of *in vivo* and *in vitro* methods have been provided to establish the bioequivalence (BE) under regulation 21CFR 320.24(b) 44 (21CFR320.1, 2015; Anand and Mitra, 2002; Greenbaum et al., 2004). The conventional *in vivo* BE study with pharmacokinetic endpoints such as Cmax and AUC is neither appropriate nor feasible for establishing BE of topically applied ophthalmic drug products. Determination of topical bioequivalence for locally acting drugs in eye is more complicated as local drug concentrations cannot be measured directly. The guidance on bioavailability and bioequivalence drafted by Committee of Proprietary Medical Products (CPMP) of the European regulatory authorities stated "for medicinal products not intended to be delivered into the general circulation, the common systemic bioavailability approach cannot be applied" (EMA, 2000). The US FDA provided certain recommendations with respect to the establishment of BE for such specific products (FDA, 2010). Draft guidance documents on locally acting topical drug products such as cyclosporine ophthalmic emulsions and acyclovir topical ointments have been developed by FDA to provide recommendations to sponsors to meet statutory and regulatory requirements (FDA, 2012, 2013). Generally, FDA addresses the issue on a case by case basis as outlined by the drug-specific guidance. Therefore, it is necessary to identify the key scientific principles for consistent and efficient identification of bioequivalence methods for locally acting topical ophthalmic drug products. The current regulation requires conducting clinical endpoint trials for demonstrating BE between topical generic and reference listed drug (RLD) products when alternative methods such as pharmacodynamics endpoint measures are not feasible (21CFR320.1, 2015; 21CFR320.24, 2015). Clinical endpoint bioequivalence studies with topical ophthalmic drug products are lengthy and expensive (Shah et al., 1998) as they are subjected to greater variability than other *in vivo* methods for determining bioequivalence. Consequently, it is not unusual that these clinical endpoint bioequivalence studies demand the enrollment of several hundred subjects to achieve sufficient statistical power (Bhandari et al., 2002; Donner and Eliasziw, 1994). Recognizing the challenges and limitations associated with the *in vivo* approach, the current study intends to establish methodologies for comparison based on *in vitro* characterizations.

Most of the studies to date have been primarily focused on ophthalmic solutions with physicochemical properties such as pH, viscosity, buffer capacity, osmolality, presence of foreign particles *etc.* The impact of physicochemical properties of ophthalmic ointments and physiological factors of the complex ocular environment on the clinical performance of the product is not well understood. The present investigation was carried out for the feasibility of using *in vitro* approach to assess the quality and performance of ophthalmic ointment, encompassing physicochemical characterizations and *in vitro* transcorneal drug permeation studies using Design of Experiments (DoE) approach. Acyclovir ointment with an oleaginous base was selected as a model dosage form in the present studies. The selections were based on existing reported use of acyclovir for the treatment of ocular Herpes Simplex Virus (HSV) keratitis, one common cause of corneal (infectious) blindness. (Tabbara and Al Balushi, 2010)

The HSV infection of the cornea is characterized by progression of viral replication in three distinct regions of the cornea: the epithelium, the stroma, and posterior region (following cornea perforation) (Grant, 1987; Liesegang et al., 1989; Sanitato et al., 1984). Acyclovir is a well-established synthetic purine nucleoside analogue with *in vitro* and *in vivo* inhibitory activity against herpes simplex virus types 1 (HSV-1), 2 (HSV-2), and varicella-zoster virus (VZV) (Acosta and Flexner, 2011). The first commercial acyclovir ophthalmic ointment was developed in 1981 with good tolerance (Grant, 1987). In the US, acyclovir ointment is only available in polyethylene glycol base (Zovirax 5%), and approved only for topical use (DailyMed, 2015). Acyclovir ophthalmic ointment (Zovirax 3%) in petrolatum base is available outside US but not yet approved for treating viral infections of the eye in the US.

The primary principle guiding the design of the current study constitutes identification of critical material attributes (CMA) and critical process parameters (CPP) influencing the critical quality attributes (CQA) of ophthalmic ointments. This will ensure that the variability of ingredients and manufacturing processes are accurately captured by discriminating *in vitro* methods. A statistical screening design (Plackett-Burman) was used to prepare various formulations with drastic difference in both design and processing. These DoE formulations were then subjected to physicochemical characterization (drug assay, content uniformity, particle size, and rheology) and *in vitro* performance tests (drug release and transcorneal drug permeation). The selection of the independent variables and the responses for the statistical design was based on the outcome of risk-analysis (omitted in the current manuscript), and only high risk ranking formulation and processing parameters, as well as CQAs were chosen. The analysis of the experimental results consisted of assessing influence of formulation and process on particular quality attributes as well as understanding the interplay of quality attributes with physiological conditions of the ocular environment, with the goal of better product and process understanding. Additionally, a novel approach of using multivariate analysis was explored to demonstrate the feasibility and potential of assessing product equivalence based on variations of various response factors.

2. Materials and methods

2.1. Materials

Acyclovir USP (>99%) were purchased from RIA International LLC (East Hanover, NJ, USA). Polyethylene glycol 400 (PEG-400), polyethylene glycol 3350 (PEG-3350), white petrolatum USP, heavy mineral oil USP, phosphate buffer saline (PBS, 10X), glacial acetic

acid USP, citric acid anhydrous, sodium chloride, and boric acid were purchased from Fischer Scientific, Norcross, GA. Lanolin alcohol (Ceralan®) was obtained from Lubrizol (Cleveland, Ohio). Unless otherwise specified, all materials were of analytical grade.

2.2. High performance liquid chromatography (HPLC) analysis of acyclovir

The HPLC system is consisted of an Agilent 1260 Series (Agilent Technologies, Wilmington, DE, US) equipped with a binary pump, online degasser, column heater, autosampler and photodiode array UV/Vis detector. Data collection and analysis were performed using ChemStation (Agilent Technologies). The current method was adopted from literature (Parry et al., 1992), and validated as per the USP <1225> and ICH Q2R1guideline. Briefly, the separation was achieved on a SunFire™ C18 column (5 μm, 4.6 mm × 150 mm). The elution was isocratic at 1.2 mL/min with a mobile phase of 0.5% (*v*/*v*) acetic acid (pH 2.8). The column temperature was maintained at 25 °C. The injection volume was 5 μL and detection was by UV at 254 nm. Linearity was established in the concentration range of 0.04 to 10 μg/mL ($r^2 = 0.999$), and the method was precise (<1% relative standard deviation for both intra- and inter-day variation) and accurate (99.8% recovery). The standard curve, constructed as described above, was used for determining the acyclovir quantity in the samples of content uniformity, drug release, cornea permeation and retention studies.

2.3. Preparation of acyclovir ointment formulations and design of experiments

Fine acyclovir particles were obtained by passing the raw API (d_{90} > 100 μm) through an air jet mill (00-Jet-O-Mizer, Fluid Energy, Telford, PA) to desired particle size (X_1, determined using HALEOS, Sympatec, Clausthal-Zellerfeld, Germany). Depending on the formulation and process design (Table 1) various quantity (X_2) of the milled API were dispersed into oleaginous ointment bases *via* melt fusion method. Briefly, weighed quantity of mineral oil (X_3) and ointment base (petrolatum, 100%-X_2–X_3) were mixed under constant stirring rate (X_4) and melted at desired temperature (X_5) controlled *via* a water bath, after which fine acyclovir particles were added into the slurry under constant stirring (X_4, mechanical mixer). Agitation was continued for an extended period of time (X_6) at the same temperature to obtain a homogeneous mixture. Ointment was then allowed to cool at various rates (X_7) to 30 °C under stirring using various outside batch temperatures. Once cooled, the ointment was packaged into multiple-dose aluminum tubes with ophthalmic tips (approx. 5 g each tube) and stored at 25 °C/60% RH until further use. Placket–Burman screening design was chosen to evaluate the impact of various factors (X_1–X_7). It is a two level screening design that involves a large number of factors and relatively few runs. Being a Resolution III design, it is only suitable for estimate of the main effects from the factors, not the interactions. The selection of the low and high values was based on the risk-analysis and preliminary study results. Investigated responses include drug assay (Y_1), content uniformity (Y_2), particle size in ointment (Y_3), rheological characteristics (yield stress Y_4, storage modulus Y_5, and high shear viscosity Y_6)), *in vitro* drug release constant (Y_7), *in vitro* transcorneal drug permeation rate constant (Y_8). Appropriate replicates (center points) were selected to obtain error estimates.

2.4. Content uniformity and drug assay

Physical characteristics of the ointment as well as its drug content were examined to assess the content uniformity of the dosage form. Briefly, three separate units of packed aluminum tubes were selected. For each unit, the bottom seal was cut off and a vertical cut was made from the bottom to the top of the tube to expose the ointment drug product. The product was inspected for any change in physical appearance and/or texture. To test for drug content, an appropriate amount of accurately weighed ointment (90–110 mg) was removed from the top, middle and bottom portions of the tube, and transferred to a flask containing 400 mL solvent (pH 9.2 borate buffer). The contents were homogenized at 8000 rpm for 15 min (50 °C), filtered (0.45 μm PVDF), diluted suitably and analyzed using HPLC for determining acyclovir concentration. Drug concentration in the top, middle and bottom portions of the ointment was calculated to analyze the uniformity of drug distribution in the ointment. Relative standard deviation of drug concentration for each DoE formulation were calculated and used for DoE statistical analysis. Drug assay was performed on additional three separate units of packed aluminum tubes, following identical procedures as in content uniformity test, with the exception that only ointment from middle portion of the tube was used for drug assay.

2.5. Particle size analysis

Ointment samples were applied onto a glass slide and spread evenly using a cover slip. Images were acquired using an Olympus BX51 polarized light microscopy (Olympus America Inc., Melville, New York). On average about 3 microscopy images (about 500–2000 particles) were acquired for each sample (200× magnification). In each image, particles were automatically counted and measured using ImageJ software (National Institute of Health, Bethesda, MD) to obtain particle size and elongation information which were then imported into Excel to generate statistical

Table 1
Plackett–Burman screening design for acyclovir oleaginous ophthalmic ointments.

Sample ID	X_1, API size (μm)	X_2, drug% (w/w)	X_3, mineral oil% (w/w)	X_4, stirring rate (rpm)	X_5, mixing temp. (°C)	X_6, mixing time (h)	X_7, cooling rate (°C/min)
DoE-1	6	6	15	2000	40	1	2.0
DoE-2	6	2	15	1000	40	2	2.0
DoE-3	38	2	0	2000	40	2	1.0
DoE-4	38	6	15	1000	40	1	1.0
DoE-5	6	2	0	2000	40	1	1.0
DoE-6	38	6	0	1000	40	2	2.0
DoE-7	17	4	7.5	1500	50	1.5	1.5
DoE-8	17	4	7.5	1500	50	1.5	1.5
DoE-9	17	4	7.5	1500	50	1.5	1.5
DoE-10	38	6	15	2000	60	2	1.0
DoE-11	38	2	15	2000	60	1	2.0
DoE-12	38	2	0	1000	60	1	2.0
DoE-13	6	6	0	1000	60	1	1.0
DoE-14	6	6	0	2000	60	2	2.0
DoE-15	6	2	15	1000	60	2	1.0

information (*i.e.*, D_{10},D_{50} and D_{90}) with a percentile function. Particle size of acyclovir API powder was determined using a HALEOS laser diffraction instrument, equipped with a R5 lens (0.5–875 μm). For each measurement, approximately 100 mg of dry sample was dispersed at a feed rate of 50% by a controlled feeder (VIBRI/L), with dry dispersal (RODOS) attachments set at a main pressure of 1.0 bar. The triggering condition was set at 0.2% optical concentration. Data were analyzed using Fraunhofer theory with WINDOX 5 software (Sympatec, Clausthal-Zellerfeld, Germany).

2.6. Rheological characterization

Rheological behaviors of ointments were evaluated using a stress-controlled hybrid rheometer (DHR-3, TA Instruments, New Castle, Delaware, USA) equipped with a step-peltier stage (25 °C) and a 25 mm sandblasted parallel plate. For each test, approximately 0.3 mL of ointment sample was placed on the lower plate, before slowly lowering the upper plate to the preset trimming gap of 550 μm. After trimming excessive material, the geometry gap was set at 500 μm. The following procedures were performed in sequence on each sample to characterize its rheological behavior: (1) 10 min equilibration (time sweep mode) to allow the material to fully recover from the shear applied during sample preparation (monitored at 0.005% strain and 1 Hz oscillation); (2) assessment of the yield stress with strain sweep method (0.005-5% strain at 1 Hz), determined by plotting storage modulus *vs.* oscillation stress and finding the onset point (Pal, 1999); (3) 10 min equilibration to allow the material to recover from the shear applied during previous step (monitored at 0.005% strain and 1 Hz oscillation); and (4) steady-state-flow method to characterize the flow property (10^{-4}–$100\ s^{-1}$) and to obtain viscosity values at low ($0.01\ s^{-1}$), medium ($1\ s^{-1}$), and high ($100\ s^{-1}$) shear rate. For the temperature sweep study, sample was first equilibrated at 16 °C for 20 min (monitored at 0.01% strain at 1 rad/s), and followed by step increase of the temperature from 16 °C to 50 °C at 1 °C interval. At each temperature, there was a 30 s soak time (equilibration time) before oscillation test was performed (0.01% strain at an angular velocity of 1 rad/s). All rheological studies were performed in triplicate and results were expressed as mean ± SD.

2.7. In vitro drug release tests (IVRT) using USP Apparatus II with enhancer cells

A modified USP Apparatus 2 equipped with 200 mL flat bottom vessels and mini paddles (Agilent Technologies, Santa Clara, CA) was used for drug release studies (Fig. 2). Excess amount of the ointment was loaded inside a special semisolid holder, Enhancer cells™ (Agilent Technologies, Santa Clara, CA) with an exposed area of 4 cm^2. Using a spatula, ointment surface was flattened, smoothed, and excess material removed, after which the exact loaded ointment quantity was determined by weight. A pre-cut and pre-wetted 0.45-μm pore size nylon membrane (Millipore, Billerica, MA) was placed over the ointment before capping the enhancer cell and removing excess water from the membrane. The capped enhancer cells were left stationary inside the empty testing vessel for 10 min to eliminate the shearing stress introduced during sample preparation and its potential impact on drug release. The pre-heated release medium (200 mL of pH 7.4 phosphate buffered saline) was transferred inside the vessel maintained at 37 °C, followed by immediate stirring of the paddle at 200 rpm. At predefined time points (5, 15, 30, 60, 120, and 240 min) aliquots of sample (0.5 mL) were withdrawn and analyzed using HPLC to determine the cumulative amount of drug release.

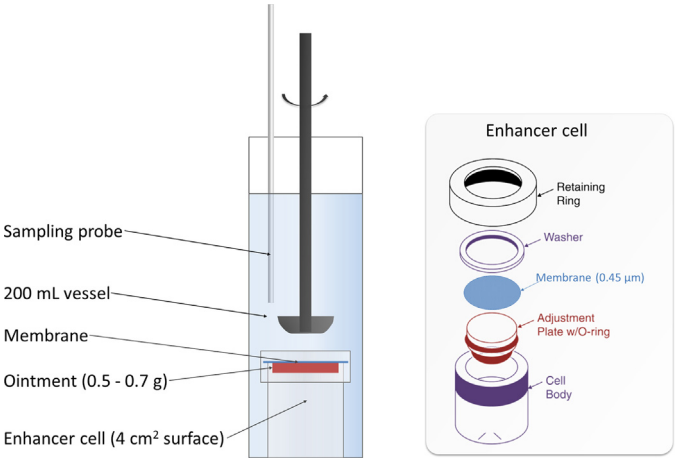

Fig. 2. *In vitro* drug release setup for ointments (USP apparatus 2 with enhancer cells).

2.8. In Vitro transcorneal drug permeation study across rabbit cornea

Fresh corneas of New Zealand albino male rabbits (Anand and Mitra, 2002) harvested within 24 h were supplied by In Vision Bio Resources (Seattle, WA). Each cornea along with 2–3 mm of sclera was individually stored in 0.75 mL of Optisol-GS (Chiron Intraoptics, Irvine, CA) within a contact lens case, and maintained at 4 °C both during (overnight) shipment and upon receiving. All corneas were used within 3 days of evisceration because of the possible damage to corneal epithelium during storage (Greenbaum et al., 2004; Means et al., 1996). *In Vitro* transcorneal drug permeation study of various oleaginous ointment formulations was carried out using vertical Franz diffusion cells with spherical joints (Perme-Gear, Inc., Hellertown, PA) (Wen et al., 2013). Prior to permeation experiment; each cornea was rinsed thrice with phosphate buffer saline (PBS, pH 7.4) to remove the residual storage solution and/or tissues. Depending on the size of the cell, 5 or 10 mL of pre-warmed PBS (pH 7.4, 37 °C) was pipetted in the receiver chamber and 200 or 400 μL in the donor chamber for equilibrating purposes. After at least 10 min, the buffer was removed from the donor chamber and excess was removed by KimWipe. The receptor chamber of the diffusion cell with exposed area of 0.20 cm^2 (capacity 5 mL) or 0.64 cm^2 (capacity 10 mL) was filled with phosphate buffered saline (PBS) and continuously stirred. The rabbit cornea with the epithelium side facing up was mounted between donor and receptor chambers. The donor chamber of the diffusion cell was filled in excess quantity of acyclovir ointment, and spread uniformly with a close-end capillary tube. The diffusion cells were thermostatically controlled at 37.0 ± 0.5 °C by means of circulating water bath. Samples of 200 μL was collected from the receiver side before adding the ointment (zero time) and at pre-determined time intervals up to 4 h and it was replaced immediately with 200 μL of warm PBS to keep the volume constant. The samples were analyzed using validated HPLC method as described above. The cumulative amount of drug permeated per surface area was calculated.

2.9. Statistical analysis

Data collected for DoE studies was analyzed using JMP software (version 11, SAS, NC, USA) with least squares fit to assess the impact of formulation and process variables. ANOVA analysis was utilized to determine the significance of the model and conduct effect analysis (Pareto charts) when appropriate.

3. Results and discussion

3.1. Drug assay and content uniformity in oleaginous ointment

Drug assay varied from 88.09% to 97.61% for fifteen DoE formulations. The ANOVA results suggested that none of the formulation and process parameters had an effect on drug assay in the prepared acyclovir ointment formulations ($F = 0.837$, Prob > $F = 0.589$).

As with many other semisolid drug products, physical separation of drug content within ointment (especially in dispersed state) may occur during both manufacturing process and shelf life conditions. Hence, it is essential to evaluate the uniformity of the finished product with respect to visual uniformity and uniformity of active ingredients, as per USP guidelines. In our study, physical segregation and/or appearance change was absent in all the examined DoE formulations, and drug content in various portion of the packaging tube did not exhibit any trend for non-uniformity (Fig. 3). Standard deviation of each DoE formulation (9 samples consisted of three tubes each determined at top, middle, bottom positions) was used as a response factor, and 7 formulation/process parameters used as independent variables to construct linear regression model using least squares method of analysis. Based on ANOVA results, the model was statistically insignificant ($F = 0.663$, Prob > $F = 0.699$) suggesting that none of the formulation and process parameters had any influence on the content uniformity of the drug substance in the oleaginous ointment.

3.2. Particle size

In the prepared oleaginous ointments, acyclovir was present in solid state as dispersed particles (Fig. 4). To determine the size and distribution of these particles, two techniques were used: laser diffraction for dry powder analysis (prior to ointment preparation) and microscopy for particles dispersed in the ointment. Different particle size values were observed for these two methods (*e.g.*, D90 of API-17 μm is 17 μm using laser diffraction and 10.4 μm using microscopy) (Table 2). This is likely a result of different measurement principles, *i.e.*, $D[1,0]$ or number mean for microscopy technique *vs.* $D[4,3]$ or volume/mass moment mean for the laser diffraction method.

With respect to formulation and process impact on the drug particle size in the final drug product, only one factor showed statistical significance (Fig. 5A): original milled API size ($p < 0.05$). However, particles present inside the final dosage from were uniformly smaller compared to the size prior to preparation (Table 2), mostly due to the grinding effect of the homogenization process. It is to be noted that in the current study, homogenization device as well as the blade was not changed, and hence the findings observed in the current study may not be extrapolated to other processes, in particular when different homogenization equipment is used.

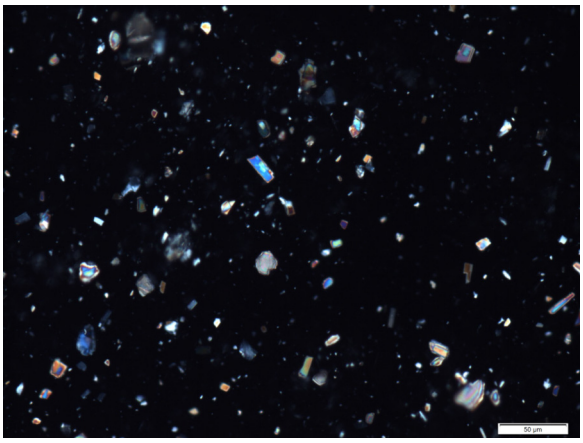

Fig. 4. Representative polarized microscopy image of acyclovir in oleaginous ointments (DoE-11, scale bar represents 50 μm length).

3.3. Rheological properties of oleaginous ointments

All of the acyclovir ointments prepared in the current study contained oleaginous base and exhibited typical viscoelastic behavior under increasing shear strain (oscillation stress/strain sweep mode). The behavior was similar to previously investigated acyclovir creams (Krishnaiah et al., 2014). Notably, both the storage (G') and loss (G'') moduli of the oleaginous ointments remained constant up to approximately 0.02–0.03% strain before declining. The region of constant modulus is generally recognized as the linear viscoelastic region (LVR), within which any disturbance to the microstructure is instantaneously recoverable. The following sections summarized the effects and implications of formulation and process variables on three notable rheological properties with

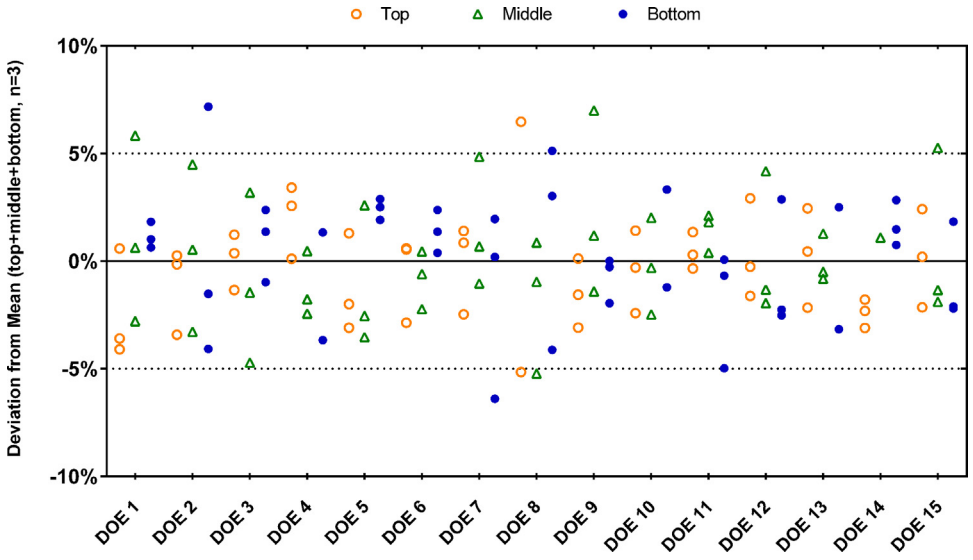

Fig. 3. Deviation from mean for DoE formulations (top, middle, and bottom portions, $n = 3$).

Table 2
Particle size and size distribution of acyclovir particles in the ointments.

Sample	Count	Length min. (μm)	Length max. (μm)	D_{10} (μm)	D_{50} (μm)	D_{90} (μm)	D_{99} (μm)
DoE-1	886	0.9	12.1	1.2 ± 0.1	2.2 ± 0.2	3.9 ± 0.1	6.7 ± 0.2
DoE-2	1435	1.0	12.1	1.3 ± 0.1	2.3 ± 0.1	4.5 ± 0.1	8.3 ± 0.7
DoE-3	2019	0.9	49.5	1.3 ± 0.1	3.2 ± 0.2	7.9 ± 0.6	19.5 ± 2.3
DoE-4	517	1.0	24.8	1.6 ± 0.3	4.0 ± 1.2	7.9 ± 1.4	16.7 ± 3.7
DoE-5	2710	0.9	19.4	1.3 ± 0.1	2.6 ± 0.2	5.6 ± 0.3	10.0 ± 0.8
DoE-6	828	1.0	27.4	1.4 ± 0.1	2.8 ± 0.3	6.9 ± 1.0	17.0 ± 3.4
DoE-7	1546	0.9	40.1	1.3 ± 0.1	2.8 ± 0.2	8.3 ± 1.0	17.8 ± 3.3
DoE-8	591	0.9	49.5	1.3 ± 0.1	2.6 ± 0.4	7.8 ± 1.6	18.5 ± 8.0
DoE-9	519	1.0	27.4	1.3 ± 0.1	3.1 ± 0.3	8.8 ± 0.4	18.1 ± 0.6
DoE-10	644	1.0	52.9	1.8 ± 0.2	4.6 ± 0.7	12.0 ± 2.5	24.0 ± 8.7
DoE-11	1099	0.9	35.9	1.4 ± 0.1	3.1 ± 0.3	8.3 ± 0.7	24.6 ± 1.7
DoE-12	914	0.9	55.6	1.5 ± 0.1	3.5 ± 0.7	8.9 ± 1.3	21.2 ± 7.0
DoE-13	2655	0.9	16.3	1.2 ± 0.1	2.5 ± 0.2	5.2 ± 0.5	10.1 ± 0.8
DoE-14	1976	0.9	18.0	1.3 ± 0.2	2.4 ± 0.5	5.0 ± 1.1	8.4 ± 1.8
DoE-15	959	0.9	15.5	1.2 ± 0.1	2.3 ± 0.3	4.7 ± 0.5	8.0 ± 1.3
API-6 μm[a]	310	0.9	21.1	1.6 ± 0.3	4.1 ± 0.5	9.2 ± 0.9	13.2 ± 3.1
API-17 μm[a]	491	0.9	37.6	1.5 ± 0.1	3.7 ± 0.4	10.4 ± 2.3	20.9 ± 4.1
API-38 μm[a]	319	1.0	38.1	2.0 ± 0.3	5.3 ± 0.4	13.7 ± 0.3	28.7 ± 1.7

[a] API particle size determined using dry powder laser diffraction (6, 17 and 38 μm are D_{90} values).

respect to their possible role in *in vivo* performance: dynamic yield stress, flow viscosity and storage modulus.

3.3.1. Dynamic yield stress

In the current study, yield stress of various DoE formulation was found to be between 51.1 and 136.0 Pa (Fig. 6A). Relative to the calculated shear stress normally present at the ocular surface (see discussion below), all of the investigated formulations would be considered easily spreadable. To assess the impact of formulation or process on the yield stress of ointment, linear regression model was applied. None of the formulation or process parameters showed a significant effect ($p > 0.05$) indicating that the observed difference in dynamic yield stress is due to random variation. This was also confirmed by ANOVA showing that the investigated model was not statistically significant ($F = 1.24$, Prob > $P = 0.393$).

When the eyelid is stationary, it exerts approximately 30 mN normal force (Ehrmann et al., 2001) over a small area of the ocular surface. Though there is still debate (Bron et al., 2011) over the exact location of the contact between the eyelid margin and the (eye) globe, one common hypothesis is that the site of action is at mucocutaneous junction (MCJ), also known as Marx's line (Ehlers, 1965; Hughes et al., 2003; Knop et al., 2011), just posterior to the gland orifice (Fig. 7). More specifically, it is an area of about 3.3 mm^2: with width of roughly 0.1 mm (Hughes et al., 2003) and span of 33 mm on the eyelid (Jones et al., 2008). Based on this information, the calculated value of tensile stress applied by the eyelid (perpendicular) to the ocular surface could be approximately 9 kPa (30 mN/3.3 mm^2). Assuming that both eyelid and ocular surface tear film can be treated as incompressible materials with a Poisson ratio (ν) of 0.5 (Jones et al., 2008; Liu and Roberts, 2005), the tensile stress could be related to shear stress in a 3:1 ratio, or roughly 3 kPa of shear stress. This shear stress is expected to increase dramatically during blinking, given the fact that the normal force increases as the eyelid moves (Ehrmann et al., 2001). In this context (Fig. 7), the yield stress values determined for the ointments provide valuable information regarding ease of spread of ointment over the ocular surface. For example, a lower yield stress (of the ointment) relative to the applied shear stress (by the eyelid) implies a higher degree of spreadability.

3.3.2. Viscosity of ointment under high shear

As shown in Fig. 6B, all oleaginous ointments exhibited non-Newtonian shear thinning viscoelastic behavior (*i.e.*, decreased viscosity with increasing shear rate), very similar to those observed in tear fluid (Rolando and Zierhut, 2001). Yet, the determined viscosity was considerably higher than the tear fluid at all shear rate range. For example, viscosity values for ointment at shear rate of 1–100 s^{-1} were 107.6 ± 24.0 Pa s and 3.3 ± 0.7 Pa s, respectively, in comparison to approximately 4 mPa s and <2 mPa s under similar conditions (Pandit et al., 1999). These results suggest that retention of ointment at the ocular surface could be significantly longer than tear fluid.

With regard to the effect of formulation and process on the viscosity, two formulation parameters were found to impact the viscosity under high shear rate: mineral oil% ($p < 0.0001$) and drug % ($p < 0.05$), as shown in Fig. 5C. Similar to the effect observed for storage modulus, variation in mineral oil content and drug particle size likely reduced the cohesiveness of the petrolatum structure, causing it to easily deform under stress. It is reasonable to expect that mineral oil reduces the cohesiveness of the petrolatum resulting in significant reduction in viscosity. Furthermore, presence of larger solid drug particles may cause friction and thereby increases the flow viscosity under shear.

To better understand the shearing effect exerted on the ointment's viscosity in a physiologically relevant context, it is important to consider the mechanical behavior and anatomy of the cornea surface. It is well known that ocular surface is covered by a thin film of complex tear fluid composed of water, enzymes, proteins, immunoglobulins, lipids, various metabolites, as well as exfoliated epithelial and polymorphonuclear cells that are constantly and dynamically changing (Rolando and Zierhut, 2001). In classical view by Wolff (Wolff, 1946), these various tear fluid components are arranged in a three-layered structure: an anterior lipid layer, an aqueous layer, and a mucin-rich layer (Fig. 7). More recent view on the structure of the tear film, however, combines the aqueous layer and mucin layer into one (aqueous-mucin layer) that exhibits a progressively low mucin concentration towards anterior lipid/air interface (Rolando and Zierhut, 2001). Nevertheless, this layer of tear film is widely considered as to not only supply all the necessary nutrients to the beneath cornea, but also to reduce friction during eyelid blinking motion (Inatomi et al., 1995), where the eyelid moves across the ocular surface at a very high speed (maximum of 17–20 cm/s (Doane, 1980)) and frequently (15–20 times per minute (Ren and Wilson, 1997)). The reported value for the thickness of the tear film varies depending on the principle of measurement, but is in the range of 3–40 μm (Bron et al., 2004; Werkmeister et al., 2013). Based

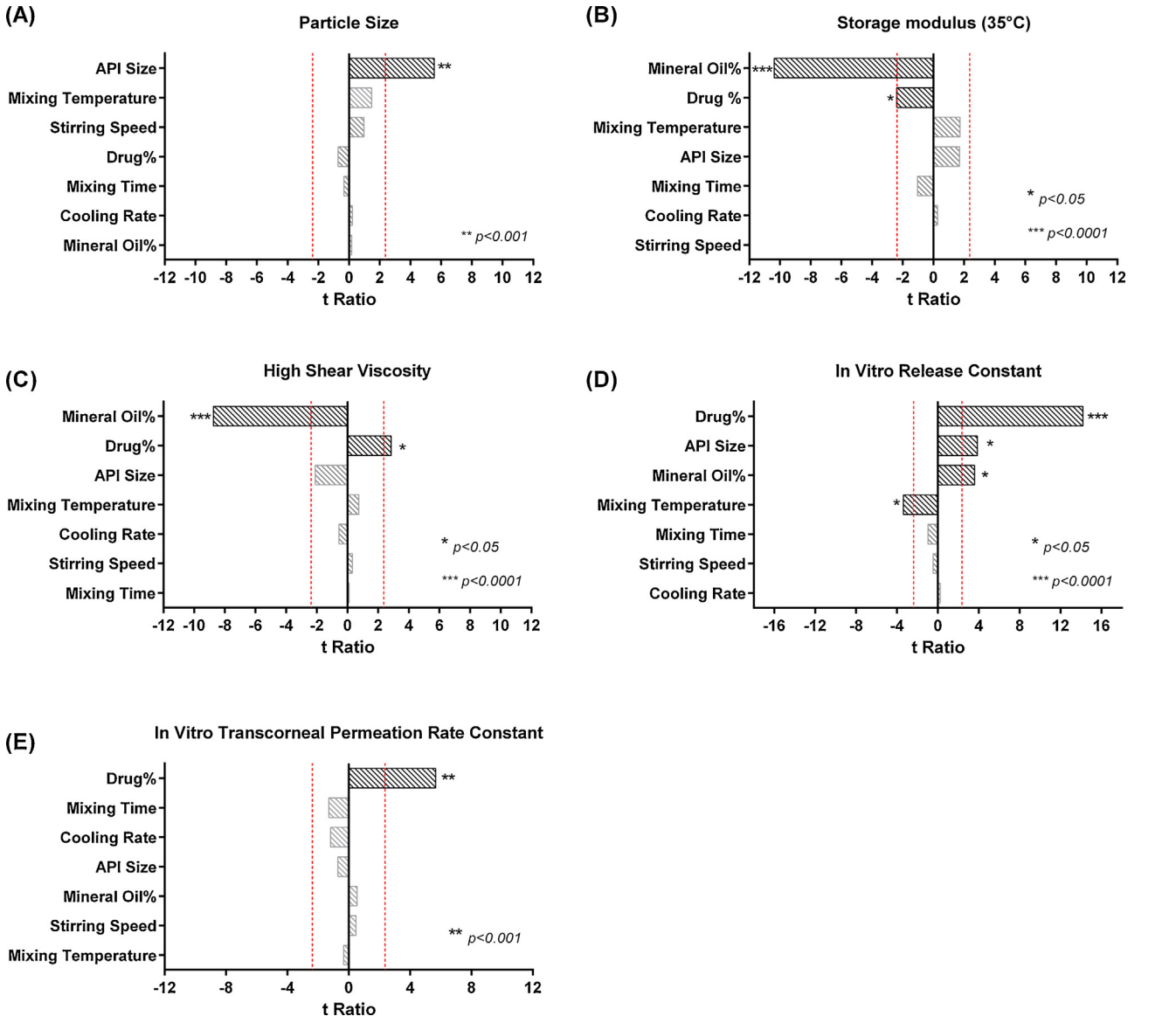

Fig. 5. Sorted parameter estimates based on *t*-ratio (high to low) for various formulation and process parameters. (A) Particle size; (B) storage modulus at 35 °C; and (C) high shear viscosity; (D) *in vitro* release constant (transient-boundary model); (E) *in vitro* transcorneal rate constant (Higuchi model).

on the eyelid velocity and tear film thickness values, the maximum shear rate exerted by the eyelid on the tear film and/or ointment samples ranges from 10^3 to $10^4\,s^{-1}$. It is difficult to determine the ointment viscosity experimentally at such a high shear rate that requires either an extremely narrow geometry gap or a very high angular velocity. In the current study, the geometry gap was chosen at 500 μm and the highest shear rate (high shear) was $100\,s^{-1}$. This represents an approximation of an early and/or later stage blinking (*e.g.*, when eyelid moves at 1–2% of the maximum velocity).

3.3.3. Storage modulus as a function of temperature

In all of the investigated oleaginous acyclovir ointments, testing (or application) temperature was found to inversely relate to both storage and loss modulus of the ointments, very similar to those observed in acyclovir creams (Krishnaiah et al., 2014). In the current study, focus was made only on the storage modulus as it pertains to the elastic component of the ointment, or cohesiveness of the micro-structure. One particular temperature of interest is at 35 °C, or ocular surface temperature (Peng et al., 2014). As shown in Fig. 6C, the storage modulus of 15 DoE ointment formulations varied from 372.3 Pa to 1285.1 Pa at 35 °C. Linear regression analysis revealed a good correlation between the factors and the response, with a correlation coefficient (r^2) of 0.9451. Further analysis with ANOVA indicated a significant effect of variables on the response ($p < 0.001$). In particular, both mineral oil% ($p < 0.0001$) and drug% ($p < 0.05$) was shown to adversely impact the storage modulus at 35 °C (Fig. 5B). Inclusion of additives such as mineral oil and/or drug particles is likely to reduce the cohesive forces within the petrolatum microstructure, and hence a negative impact on the storage modulus (elasticity).

3.4. In vitro drug release testing of (IVRT) oleaginous ointments

The acyclovir release profile of all 15 DoE formulations followed logarithmic time dependent release (Eq. (1)) rather than the typical Higuchi release (Higuchi, 1961) as shown in Fig. 8A (DoE-1 formulation as representative) and Table 3. The fundamental cause of logarithmic time dependent drug release kinetics in IVRT is likely due to the expanding Transient-Boundary at the interface of oleaginous ointment and aqueous medium (Xu et al., 2015). For a

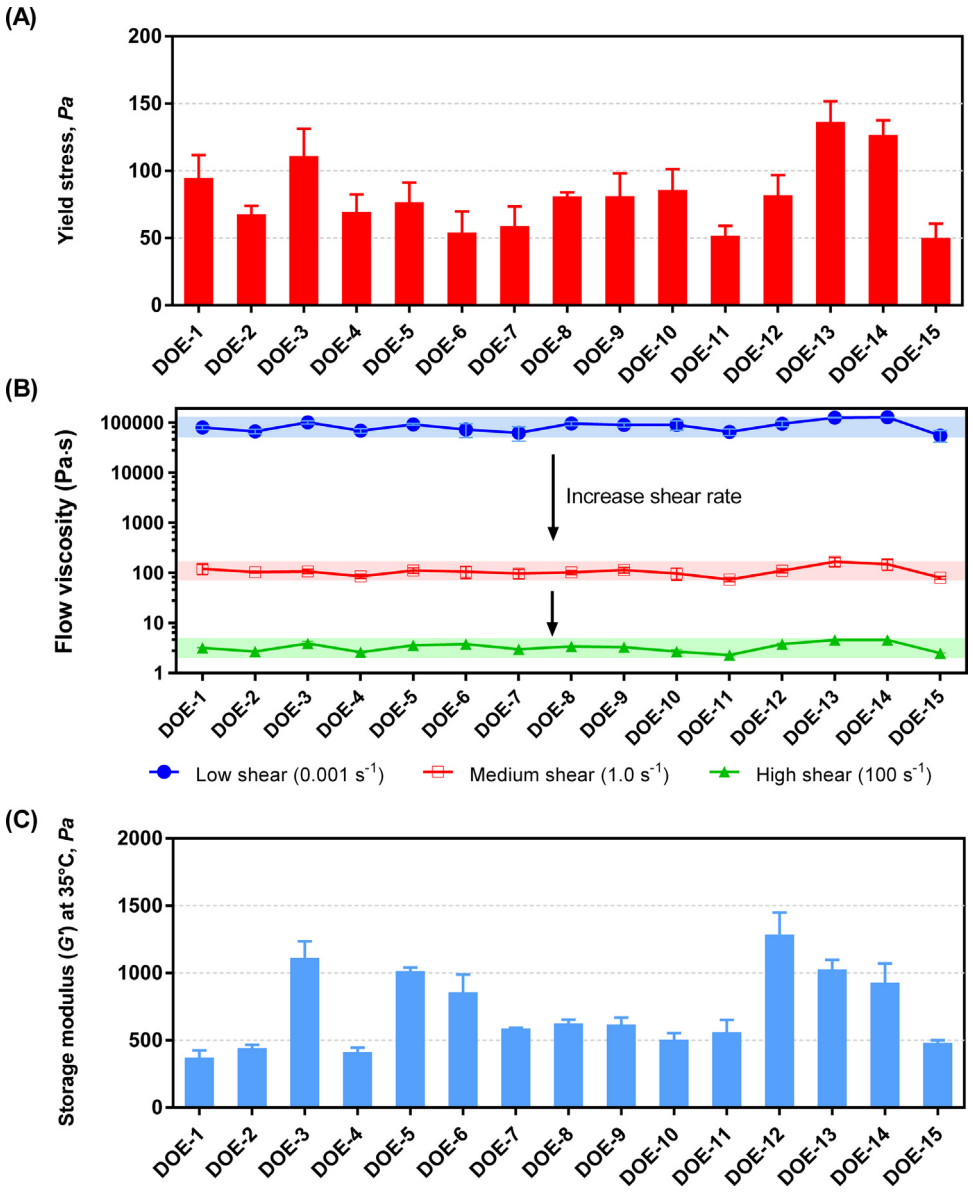

Fig. 6. Rheological characteristics of various DoE ointment formulations. (A): Yield stress; (B): viscosity at low (0.001 s^{-1}), medium (1 s^{-1}), and high (100 s^{-1}) shear rate; (C): storage modulus at 35 °C.

more detailed discussion about the theoretical basis of this Transient-Boundary, please refer to the previously published article. In brief, the drug release kinetics from oleaginous ointments was described by the following equations:

$$Q_{aq} = 2.303 \times K \times \log_{10}(t) + Q' \quad (1)$$

$$\text{and} K = \frac{D \times m \times h \times A}{v \times l} \quad (2)$$

where Q_{aq} = amount of cumulative drug released in the aqueous medium (μg), K = release constant (μg), or the slope of the Q_{aq} *vs.* base-10 logarithm of time divided by 2.303, D = Stokes–Einstein diffusion coefficient (cm^2/s), m = concentration of acyclovir (solid state) in petrolatum base ($\mu g/cm^3$), h = initial transient boundary layer thickness (μm), A = exposed surface area (cm^2), v = zero-order expansion velocity of the transient-boundary (cm/s), and l = pseudo steady state diffusion thickness (μm). Since the exposed surface area (A) is always a constant (*i.e.*, filter membrane size), all of the cumulative release amount or slope has been normalized to unit surface area numbers, *i.e.*, Q_{aq}/A and K/A, in the unit of $\mu g/cm^2$.

In the current study, the unit area release constant (K/A) for 15 DoE formulations varied from 0.664 to 3.339 $\mu g/cm^2$ (Table 3). A good correlation was found between the formulation/process parameters and the drug release constant with a correlation coefficient (r^2) of 0.9718. The ANOVA confirmed that the correlation was statistically significant ($p < 0.0001$). More detailed effect analysis revealed that drug release from oleaginous ointment is predominantly influenced by formulation design (Fig. 6D), where drug% ($p < 0.0001$), API size, and mineral oil% can all significantly impact the drug release (in decreasing order); On the process side, mixing temperature, which indirectly influenced the rheological behavior of the ointment base, was identified as the most important process parameter ($p < 0.05$).

For convenience of sample preparation, drug% used in the formulation design describes the weight-by-weight percentage of acyclovir (solid) relative to the total ointment mass, including petrolatum with or without mineral oil. This is essentially the same

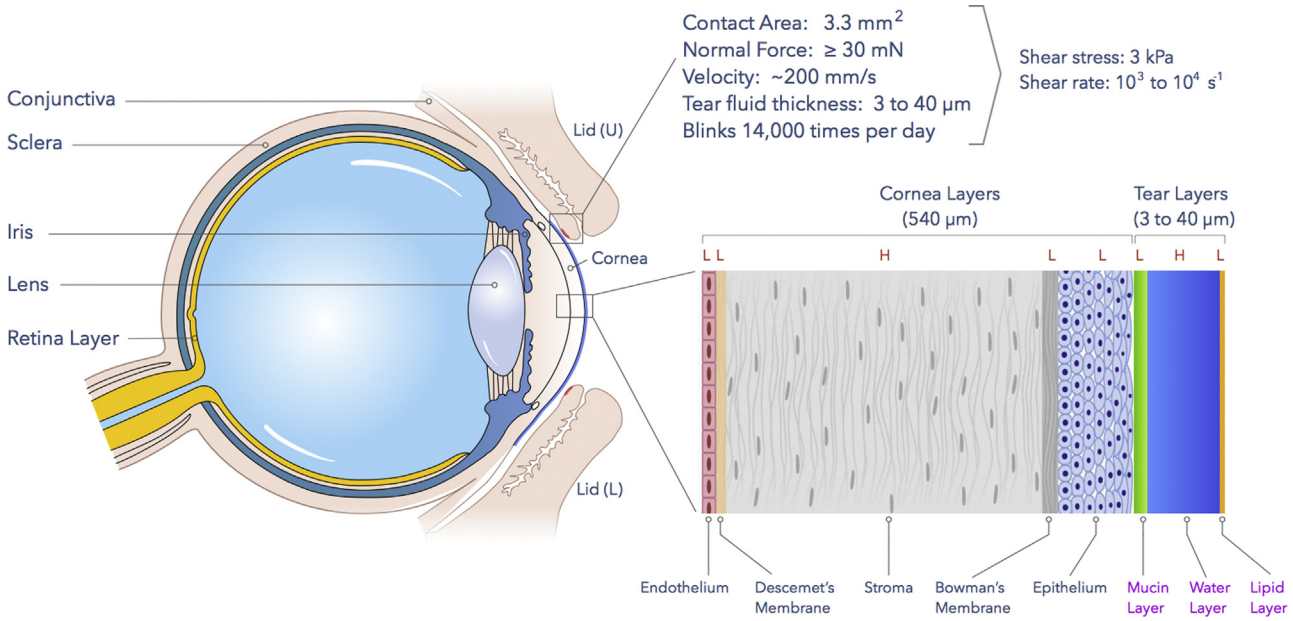

Fig. 7. Role of ocular surface in the evaluation of ointment formulation.

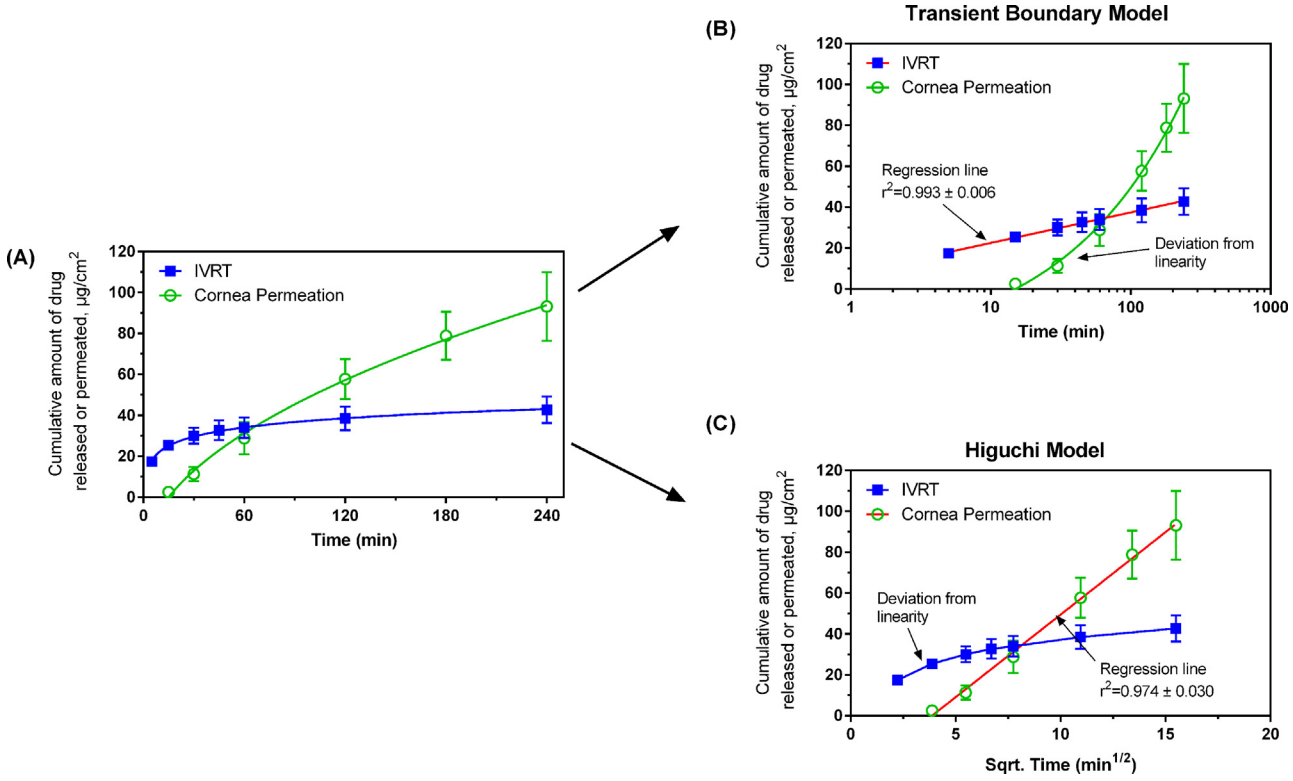

Fig. 8. *In vitro* drug release and transcorneal drug permeation from acyclovir DoE-1 formulation ($n = 6$): (A) Cumulative amount of drug released/permeated per unit area in linear time scale; (B) cumulative amount of drug released/permeated per unit area fitted with transient-boundary model; and (C) cumulative amount of drug released/permeated per unit area fitted with Higuchi model. (For interpretation of the references to color in the text, the reader is referred to the web version of this article.)

as the drug concentration (m) used in the Transient-Boundary Model (Eq. (2)), expressed on a weight-by-volume basis (interchangeable *via* density of the ointment base). Logically, higher concentration of the drug (solid state) in the initial boundary layer can lead to higher concentration of the solubilized drug (molecular state) in the transient layer, and consequently a greater drug release. Particle size of the API is believed to have an influence on initial boundary layer thickness (h) which is expected to be in the micron size range. A large drug particle that is similar or greater than the thickness of the boundary may artificially expand the initial boundary layer thickness (analogy to transmembrane protein relative to the membrane). Mineral oil% is likely to have an effect on the drug release by indirectly accelerating drug diffusion (D) as it reduces the viscosity of the petrolatum, particularly at the ointment/water interface, in similar way as the mixing temperature effect.

Table 3
Kinetics of *in vitro* drug release from various DoE formulations ($n = 6$).

Formulation	Zero order		First order		Higuchi model		Transient-boundary model	
	k_0	r^2	k_1	r^2	k_H/A	r^2	K/A	r^2
DoE-1	0.086 ± 0.020	0.718 ± 0.062	−0.003 ± 0.000	0.593 ± 0.067	1.751 ± 0.424	0.884 ± 0.043	6.484 ± 1.611	0.993 ± 0.006
DoE-2	0.027 ± 0.011	0.727 ± 0.078	−0.002 ± 0.000	0.643 ± 0.093	0.552 ± 0.239	0.889 ± 0.054	2.046 ± 0.942	0.986 ± 0.006
DoE-3	0.031 ± 0.007	0.813 ± 0.044	−0.004 ± 0.001	0.635 ± 0.035	0.618 ± 0.136	0.942 ± 0.03	2.199 ± 0.459	0.980 ± 0.014
DoE-4	0.103 ± 0.013	0.731 ± 0.103	−0.003 ± 0.001	0.608 ± 0.108	2.087 ± 0.252	0.891 ± 0.076	7.689 ± 0.990	0.987 ± 0.015
DoE-5	0.022 ± 0.004	0.808 ± 0.048	−0.002 ± 0.000	0.723 ± 0.051	0.429 ± 0.087	0.943 ± 0.027	1.530 ± 0.316	0.982 ± 0.011
DoE-6	0.077 ± 0.008	0.708 ± 0.066	−0.003 ± 0.001	0.587 ± 0.042	1.575 ± 0.171	0.876 ± 0.048	5.851 ± 0.650	0.989 ± 0.011
DoE-7	0.044 ± 0.006	0.728 ± 0.048	−0.002 ± 0.000	0.626 ± 0.057	0.884 ± 0.122	0.887 ± 0.032	3.258 ± 0.472	0.987 ± 0.008
DoE-8	0.046 ± 0.009	0.730 ± 0.092	−0.002 ± 0.000	0.622 ± 0.092	0.937 ± 0.176	0.888 ± 0.068	3.438 ± 0.587	0.986 ± 0.014
DoE-9	0.050 ± 0.016	0.790 ± 0.106	−0.003 ± 0.001	0.680 ± 0.133	0.991 ± 0.273	0.914 ± 0.038	3.506 ± 0.816	0.959 ± 0.082
DoE-10	0.084 ± 0.012	0.761 ± 0.040	−0.004 ± 0.001	0.600 ± 0.063	1.701 ± 0.246	0.915 ± 0.027	6.200 ± 0.913	0.997 ± 0.001
DoE-11	0.026 ± 0.006	0.742 ± 0.092	−0.003 ± 0.001	0.628 ± 0.107	0.524 ± 0.124	0.897 ± 0.068	1.921 ± 0.478	0.984 ± 0.014
DoE-12	0.031 ± 0.007	0.789 ± 0.080	−0.003 ± 0.000	0.693 ± 0.093	0.614 ± 0.148	0.931 ± 0.047	2.212 ± 0.561	0.986 ± 0.014
DoE-13	0.057 ± 0.006	0.813 ± 0.057	−0.0020 ± 0.001	0.737 ± 0.060	1.123 ± 0.116	0.945 ± 0.035	4.009 ± 0.448	0.986 ± 0.008
DoE-14	0.059 ± 0.007	0.765 ± 0.058	−0.0030 ± 0.000	0.658 ± 0.059	1.195 ± 0.140	0.916 ± 0.037	4.348 ± 0.547	0.992 ± 0.008
DoE-15	0.024 ± 0.001	0.837 ± 0.024	−0.0030 ± 0.000	0.748 ± 0.029	0.465 ± 0.023	0.963 ± 0.013	1.639 ± 0.085	0.982 ± 0.009

**Note* to the reviewer: the *K*/*A* values were updated. The values reported before was mistakenly divided by 2.303 (to correct for LN to log conversion which was already corrected, *i.e.*, divided twice).

3.5. In vitro transcorneal drug permeation

The amount of drug permeated (per unit area) from various oleaginous ointments across the rabbit cornea was determined. Fig. 8 (green open circle curve) illustrates the permeation profile of one exemplary formulation (DoE-1). All 15 DoE formulations exhibited similar permeation profile with the calculated K_H/A and r^2 summarized in Table 4. It is evident that the permeation profile of acyclovir across the cornea followed Higuchi kinetics, *i.e.*, linear with respect to square-root of time. This contrasts the IVRT profile (overlay in Fig. 8) where logarithmic time model fits better than Higuchi model. Furthermore, at the end of 4 h, amount of acyclovir permeated across cornea was more than the amount of drug released. This contrasting difference could be explained based on the differences in the physical boundary conditions (Fig. 9) of *in vitro* drug release and *in vitro* transcorneal drug permeation studies.

Upon close examination of the theoretical basis of the two models (*i.e.*, Higuchi and Transient-Boundary models), in particular the assumptions about the role/function of the interfacial boundary, it is speculated that the differences observed in two *in vitro* experiments is due to change in the physical boundary conditions. For example, in the IVRT situation, the physical boundary between ointment and water is more clearly defined (Fig. 9A), as the ointment and water are inherently immiscible to each other. Drug release occurs as a result of "surface drug" solubilization as well as the boundary expansion (towards the release medium) as discussed earlier. However, with respect to drug release and drug permeation on the surface of cornea, presence of cornea epithelium cells (Fig. 9B) as well as the tear film (Fig. 9C) may change the boundary condition. Since both the top layer of the cornea epithelium and the tear film is lipophilic in nature, petrolatum-based ointment may have greater interaction with epithelium during *in vitro* drug permeation across the cornea relative to the IVRT experiment, and may consequently lead to higher amount of drug permeation. Initial delay in drug permeation (Fig. 8A) is likely a result of lag time between drug release from ointment and permeation through cornea. Based on these interesting findings, further studies have been carried out to find the effect of ointment base type on the corneal drug permeation, and results will be reported in another publication.

With respect to formulation and process impact on acyclovir permeation across cornea, only drug% showed a statistical significance ($p < 0.001$) (Fig. 5E). This is likely due to the impact of drug% on drug release. As shown early, drug% was the most significant parameter affecting drug release (IVRT). Despite the differences in the release kinetics (Transient-Boundary *vs.* Higuchi), higher amount of drug (solid state) present inside the ointment is believed to result in greater drug release, and

Table 4
In vitro transcorneal drug permeation from DoE formulations ($n = 6$).

Formulation	Cumulative amount of drug permeation fitted using Higuchi model	
	k_H/A	r^2
DoE-1	8.073 ± 1.026	0.974 ± 0.030
DoE-2	1.635 ± 0.827	0.990 ± 0.005
DoE-3	1.883 ± 0.396	0.993 ± 0.006
DoE-4	5.556 ± 1.708	0.994 ± 0.003
DoE-5	1.655 ± 0.676	0.983 ± 0.019
DoE-6	5.267 ± 0.764	0.989 ± 0.011
DoE-7	3.497 ± 0.919	0.982 ± 0.025
DoE-8	6.296 ± 1.537	0.998 ± 0.002
DoE-9	3.862 ± 1.577	0.984 ± 0.025
DoE-10	4.435 ± 0.614	0.974 ± 0.045
DoE-11	2.698 ± 1.767	0.950 ± 0.097
DoE-12	2.467 ± 0.790	0.988 ± 0.012
DoE-13	5.489 ± 0.568	0.985 ± 0.021
DoE-14	5.607 ± 1.710	0.992 ± 0.008
DoE-15	2.085 ± 0.416	0.981 ± 0.016

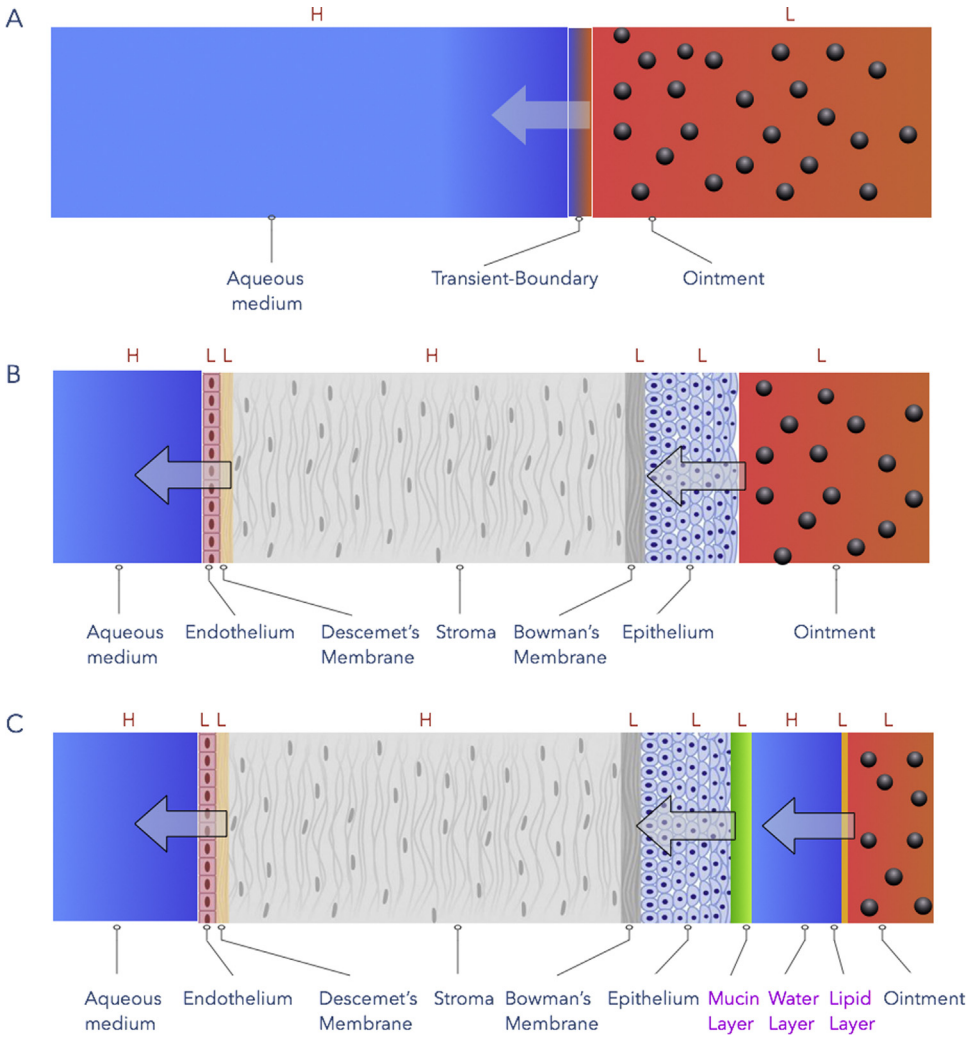

Fig. 9. Differences in the drug release interface and their impact on drug transport process. (A) *in vitro* drug release, (B) *in vitro* transcorneal drug permeation and (C) possible occurrence of *in vivo* transcorneal drug permeation. *L* and *H* were used to indicate the lipophilic and hydrophilic nature of the layers, respectively.

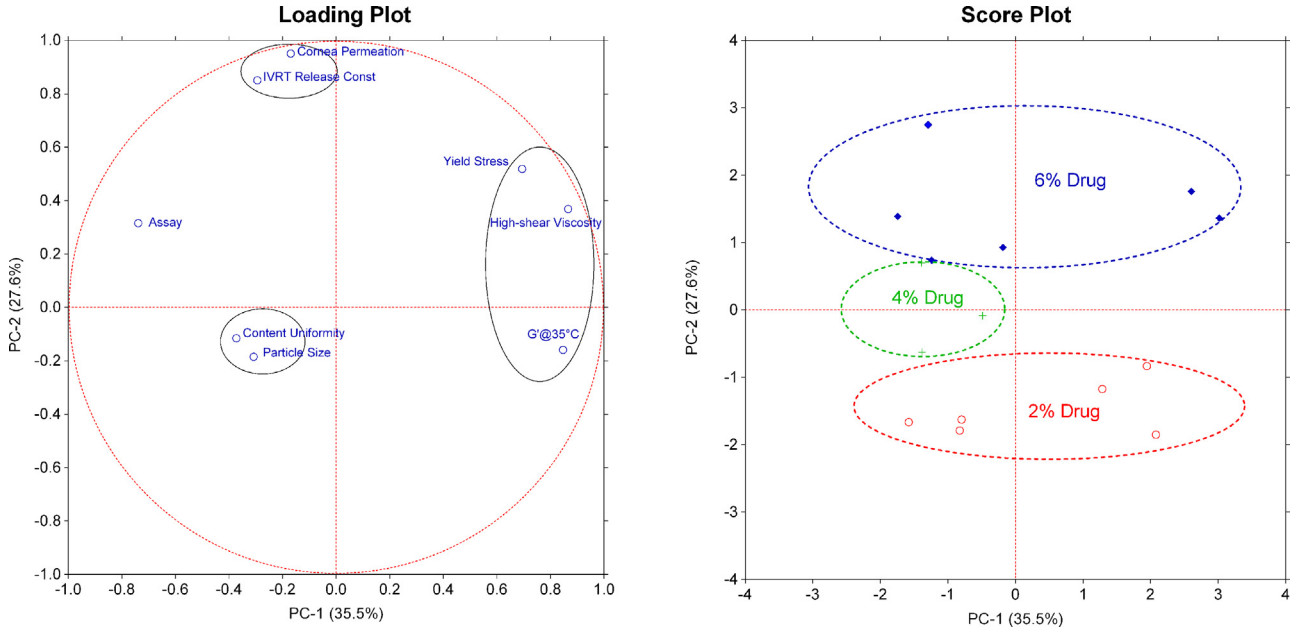

Fig. 10. PCA analysis results: correlation loading plot (left) and score plot (right) of first two principle components for various responses (mean center and scale). In score plot, 15 DoE samples are highlighted based on drug% (blue diamond: 6%; green cross: 4%; red circle: 2%). (For interpretation of the references to color in this figure legend, the reader is referred to the web version of this article.)

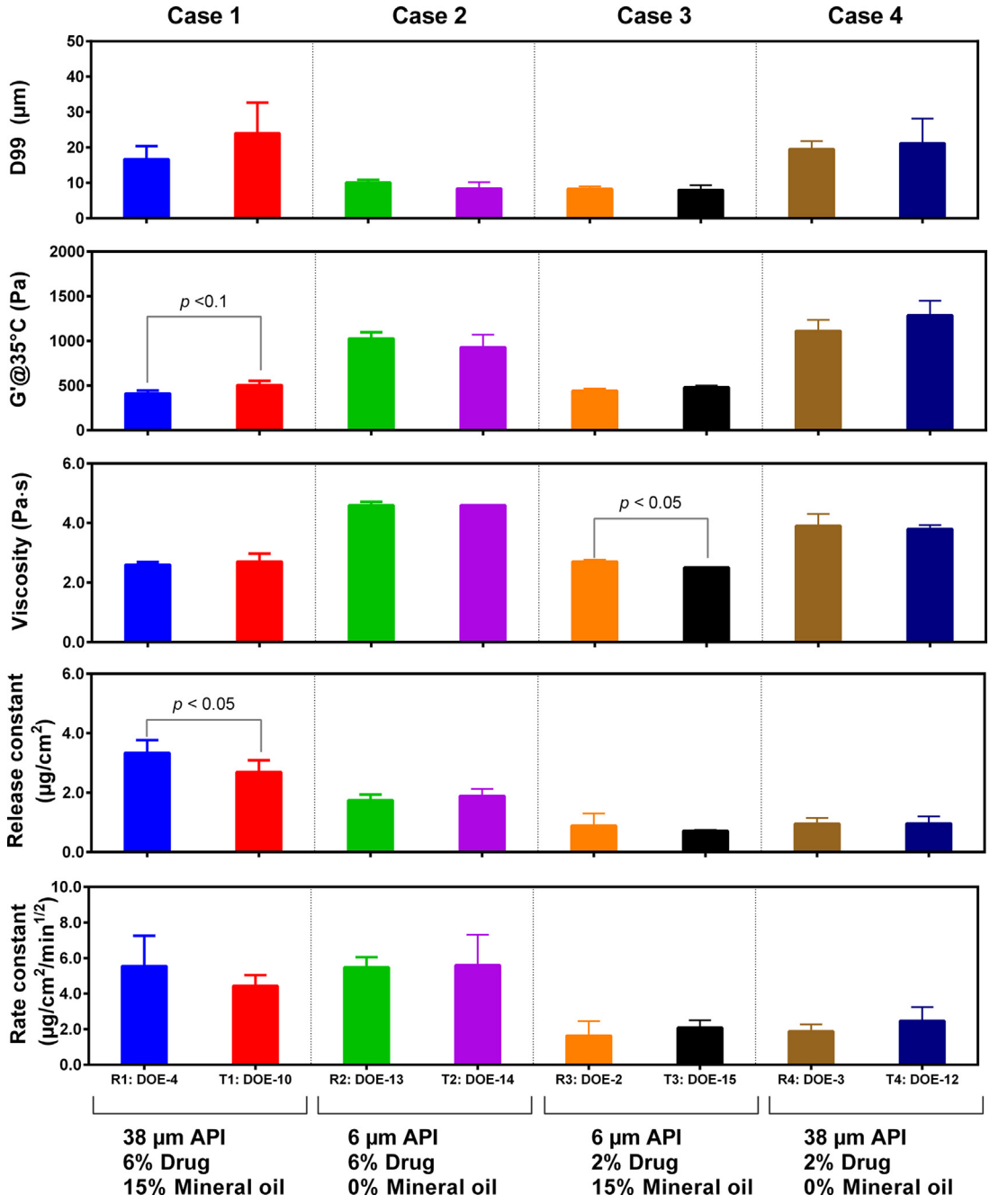

Fig. 11. Case studies on *in vitro* comparison of four pairs of Q1/Q2 equivalent formulations.

consequently higher drug permeation (concentration dependent diffusion process) across the cornea.

3.6. Principle component analysis to identify the critical quality attributes

In the current study, out of the 8 evaluated formulation characteristics (*i.e.*, assay, content uniformity, particle size, yield stress, storage modulus at 35 °C, shear viscosity, *in vitro* drug release and transcorneal drug permeation), five were found to be sensitive to formulation and/or process variations (Fig. 5). In the section below, attempts were made to assess all of the investigated responses from a difference perspective, where variation of the multivariable responses is the focus rather than the effect of independent formulation and/or process parameters. This type of multivariate analysis has been widely used for spectroscopic analysis (chemometrics), and in recent years extended with much wider applications. (Escandar et al., 2006; Lavine and Workman, 2010), Principle component analysis (PCA) was used to decomposing the information (variations of the responses) into a set of components (or latent variables) such that the first component accounted for as much of the variation in the data as possible, the second component accounted for the second largest variation, and so on. Moreover, each component in the analysis was orthogonal to each other; that is, each component was uncorrelated with the others: as a direction in space, each component was at right angles to the others.

Due to the scale differences among variables (*e.g.*, content uniformity values are less than 10% while storage modulus are greater than 100 Pa), all 8 variables underwent a preprocessing

(mean center and scale with standard deviation) before applying PCA. Fig. 10 shows the correlation loading plot of first two principle components (when combined accounts for 63% of the variations). Notably, yield stress, high shear viscosity and G' at 35 °C were distributed in the same hemisphere, correlating to first principle component (PC-1). In particular, high shear viscosity and storage modulus accounted for more than 80% of variations in PC-1. On the other hand, IVRT release constant and corneal drug permeation rate constant clustered together, and both highly related to PC-2 (accounts for >80% variations). As with other multivariate analysis, the exact physical meanings of PC-1 and PC-2 are difficult to interpret. However, in this study, the locations of the responses suggested that PC-1 and PC-2 were related to rheological characteristics and drug concentration of the ointment system, respectively. Using similar principle, it can be speculated that content uniformity, particle size of the drug, as well as assay are relatively less critical in response to formulation and process changes. It should be noted that the variations introduced in the current study represents extreme scenarios (*e.g.*, change the component ratio as much as 15% and vary the agitation speed as much as 100%). To assess the criticality of response (quality attributes) under normal manufacturing conditions, actual manufacturing data is needed. It is further cautioned that the PCA model constructed in Fig. 10 is based on relative small data set and larger data sets are preferred to further improve the usefulness of the model. Nonetheless, this PCA model provided similar observation as did the DoE analysis indicating that *in vitro* drug release, corneal drug permeation, and rheological characterizations were critical quality attributes, under the investigated conditions.

3.7. Establishing product sameness based on Q1/Q2/Q3 criterion

Establishment of therapeutic equivalence of complex generic drug products such as locally acting ophthalmic ointments is challenging. However, like other similar cases (FDA, 2012, 2013), it may be possible to establish equivalence based on *in vitro* methods when no other alternative approach provides better information and when product having the same components (Q1) and same composition (Q2) as well as the same characteristics (or microstructures) (Q3) can provide high level of confidence of product sameness. In discussion below, 8 DoE formulations were grouped into four pairs (Case 1 to Case 4) where within each pair two formulations had identical components and composition (Q1/Q2 equivalent) but differed in processing conditions (case 1: differed in stirring rate, mixing temperature, and mixing time; case 2: differed in stirring rate, mixing time, and cooling rate; case 3: differed in mixing temperature and cooling rate; Case 4: differed in stirring rate, mixing temperature, mixing time, and cooling rate).

Using five identified CQAs, it was found that in two cases (cases 2 and 4), the two formulations showed no difference in all five qualities, albeit changes in their respective processing conditions (Fig. 11). In contrast, in cases 1 and 3, the two formulations exhibited differences in terms of rheology and/or *in vitro* drug release. Consequently in these two cases the test product may not be considered same as the reference product. It is to be cautioned, however, that due to the limitation of the screening design (Plackett–Burman), the comparison of the formulation sameness as illustrated in Fig. 11 was not ideal. The formulation variables should have been kept constant to ensure Q1/Q2 sameness in order for the Q3 evaluation (Krishnaiah et al., 2014; Rahman et al., 2014). Furthermore, for equivalence evaluation, ideally T/R ratio would be needed as per USP guideline (USP38-NF33, 2015). However, due to the lack of true reference product in this study, such evaluation was not possible.

4. Conclusions

Design of experiments and principle component analysis approaches were used in this work to identify the effect of various critical formulation and process parameters on the product quality and performance. Strength of the drug substance in the final ointment formulations (or drug loading) was found to be the most influential formulation parameter in a variety of investigated responses including rheological characteristics of the ointments, *in vitro* drug release, as well as *in vitro* transcorneal drug permeation. Processing had minor impact on the rheological properties of the acyclovir ointments. The results suggested that the *in vitro* approaches used in determining API particle size, storage modulus of ointment, high shear viscosity of ointment, *in vitro* drug release constant and *in vitro* transcorneal drug permeation rate constant were able to discriminate the product and process variability, and to evaluate product sameness. Of special importance, interfacial boundary conditions were found to play crucial role in the drug transport process, including the *in vitro* drug release, *in vitro* transcorneal drug permeation, and potentially under *in vivo* corneal conditions too. With a good understanding of the anatomy and physiology of the eye, ophthalmic formulations with precisely measured *in vitro* properties has the potential to exhibit sameness for equivalence determination between two products.

Appendix A. Supplementary data

Supplementary data associated with this article can be found, in the online version, at http://dx.doi.org/10.1016/j.ijpharm.2015.07.066.

References

21CFR320.1, 2015. Title 21: Food and Drugs: Part 320—Bioavailability and Bioequivalence Requirements, Subpart A—General Provisions. Available at http://www.ecfr.gov/cgi-bin/text-idx?SID=301bbb87cfab41036bc82f497f1aa9aa&node=pt21.5.320&rgn=div5#se21.5.320_121 (accessed 30.03.14.).

21CFR320.24, 2015. Title 21: Food and Drugs: Part 320—Bioavailability and Bioequivalence Requirements, Subpart B—Procedures for Determining the Bioavailability or Bioequivalence of Drug Products. Available at http://www.ecfr.gov/cgi-bin/text-idx?SID=301bbb87cfab41036bc82f497f1aa9aa&node=pt21.5.320&rgn=div5#se21.5.320_124 (accessed 30.03.14.).

Acosta, E.P., Flexner, C., 2011. Chapter 58: antiviral agents (nonretroviral), In: Brunton, L.L., Chabner, B.A., Knollmann, B.C. (Eds.), Goodman & Gilman's The Pharmacological Basis of Therapeutics. twelfth ed. McGraw Hill, New York (accessed 22.04.14.).

Anand, B., Mitra, A., 2002. Mechanism of corneal permeation of L-valyl ester of acyclovir: targeting the oligopeptide transporter on the rabbit cornea. Pharm. Res. 19, 1194–1202.

Bhandari, M., Lochner, H., Tornetta, P., 2002. Effect of continuous *versus* dichotomous outcome variables on study power when sample sizes of orthopaedic randomized trials are small. Arch. Orthop. Trauma Surg. 122, 96–98.

Bron, A.J., Tiffany, J.M., Gouveia, S.M., Yokoi, N., Voon, L.W., 2004. Functional aspects of the tear film lipid layer. Exp. Eye Res. 78, 347–360.

Bron, A.J., Yokoi, N., Gaffney, E.A., Tiffany, J.M., 2011. A solute gradient in the tear meniscus. I. A hypothesis to explain Marx's line. Ocul. Surf. 9, 70–91.

DailyMed, 2015. Product Label: Zovirax (Acyclovir Ointment 5%). U.S. National Library of Medicine, DailyMed.

Doane, M.G., 1980. Interactions of eyelids and tears in corneal wetting and the dynamics of the normal human eyeblink. Am. J. Ophthalmol. 89, 507–516.

Donner, A., Eliasziw, M., 1994. Statistical implications of the choice between a dichotomous or continuous trait in studies of interobserver agreement. Biometrics 50, 550–555.

Ehlers, N., 1965. The precorneal film. Biomicroscopical, histological and chemical investigations. Acta Ophthalmol. Suppl. 81, 81–134.

Ehrmann, K., Francis, I., Stapleton, F., 2001. A novel instrument to quantify the tension of upper and lower eyelids. Cont. Lens Anterior Eye 24, 65–72.

EMA, 2000. Committee for Proprietary Medicinal Products: Note for Guidance on the Investigation of Bioavailability and Bioequivalence. Available at http://www.ema.europa.eu/docs/en_GB/document_library/Scientific_guideline/2009/09/WC500003519.pdf (accessed 30.03.14.).

Escandar, G.M., Damiani, P.C., Goicoechea, H.C., Olivieri, A.C., 2006. A review of multivariate calibration methods applied to biomedical analysis. Microchem. J. 82, 29–42.

FDA, 2010. Guidance for Industry Bioequivalence Recommendations for Specific Products. Available at http://www.fda.gov/downloads/Drugs/GuidanceComplianceRegulatoryInformation/Guidances/UCM072872.pdf (accessed 30.03.14.).
FDA, 2012. Draft Guidance on Acyclovir. Available at http://www.fda.gov/downloads/Drugs/GuidanceComplianceRegulatoryInformation/Guidances/UCM296733.pdf (accessed 19.05.15.).
FDA, 2013. Draft Guidance on Cyclosporine. Available at http://www.fda.gov/downloads/Drugs/GuidanceComplianceRegulatoryInformation/Guidances/UCM358114.pdf (accessed 30.03.15.).
Gaudana, R., Ananthula, H., Parenky, A., Mitra, A., 2010. Ocular drug delivery. AAPS J. 12, 348–360.
Grant, D.M., 1987. Acyclovir (zovirax) ophthalmic ointment: a review of clinical tolerance. Curr. Eye Res. 6, 231–235.
Greenbaum, A., Hasany, S.M., Rootman, D., 2004. Optisol *vs* dexsol as storage media for preservation of human corneal epithelium. Eye 18, 519–524.
Higuchi, T., 1961. Rate of release of medicaments from ointment bases containing drugs in suspension. J. Pharm. Sci. 50, 874–875.
Høvding, G., 1989. A comparison between acyclovir and trifluorothymidine ophthalmic ointment in the treatment of epithelial dendritic keratitis. Acta Ophthalmol. (Cph.) 67, 51–54.
Hughes, C., Hamilton, L., Doughty, M.J., 2003. A quantitative assessment of the location and width of Marx's line along the marginal zone of the human eyelid. Optom. Vis. Sci. 80, 564–572.
Inatomi, T., Spurr-Michaud, S., Tisdale, A.S., Gipson, I.K., 1995. Human corneal and conjunctival epithelia express MUC1 mucin. Invest. Ophthalmol. Vis. Sci. 36, 1818–1827.
Jones, M.B., Fulford, G.R., Please, C.P., McElwain, D.L.S., Collins, M.J., 2008. Elastohydrodynamics of the eyelid wiper. Bull. Math. Biol. 70, 323–343.
Katami, M., 1991. Corneal transplantation—immunologically privileged status. Eye 5, 528–548.
Knop, E., Knop, N., Zhivov, A., Kraak, R., Korb, D.R., Blackie, C., Greiner, J.V., Guthoff, R., 2011. The lid wiper and muco-cutaneous junction anatomy of the human eyelid margins: an *in vivo* confocal and histological study. J. Anat. 218, 449–461.
Krishnaiah, Y.S.R., Xu, X., Rahman, Z., Yang, Y., Katragadda, U., Lionberger, R., Peters, J. R., Uhl, K., Khan, M.A., 2014. Development of performance matrix for generic product equivalence of acyclovir topical creams. Int. J. Pharm. 475, 110–122.
Lavine, B., Workman, J., 2010. Chemometrics. Anal. Chem. 82, 4699–4711.
Le Discorde, M., Moreau, P., Sabatier, P., Legeais, J.-M., Carosella, E.D., 2003. Expression of HLA-G in human cornea, an immune-privileged tissue. Hum. Immunol. 64, 1039–1044.
Liesegang, T.J., Melton III, L.J., Daly, P.J., Ilstrup, D.M., 1989. Epidemiology of ocular herpes simplex: incidence in rochester, minn, 1950 through 1982. Arch. Ophthalmol. (Chic.) 107, 1155–1159.
Liu, J., Roberts, C.J., 2005. Influence of corneal biomechanical properties on intraocular pressure measurement: quantitative analysis. J. Cataract Refract. Surg. 31, 146–155.
Means, T.L., Geroski, D.H., L'Hernault, N., Grossniklaus, H.E., Kim, T., Edelhauser, H.F., 1996. The corneal epithelium after Optisol-GS storage. Cornea 15, 599–605.
Pal, R., 1999. Yield stress and viscoelastic properties of high internal phase ratio emulsions. Colloid Polym. Sci. 277, 583–588.
Pandit, J.C., NagyovÁ, B., Bron, A.J., Tiffany, J.M., 1999. Physical properties of stimulated and unstimulated tears. Exp. Eye Res. 68, 247–253.
Parry, G.E., Dunn, P., Shah, V.P., Pershing, L.K., 1992. Acyclovir bioavailability in human skin. J. Invest. Dermatol. 98, 856–863.
Peng, C.-C., Cerretani, C., Braun, R.J., Radke, C.J., 2014. Evaporation-driven instability of the precorneal tear film. Adv. Colloid Interface Sci. 206, 250–264.
Rahman, Z., Xu, X.M., Katragadda, U., Krishnaiah, Y.S.R., Yu, L., Khan, M.A., 2014. Quality by design approach for understanding the critical quality attributes of cyclosporine ophthalmic emulsion. Mol. Pharm. 11, 787–799.
Ren, H., Wilson, G., 1997. The effect of a shear force on the cell shedding rate of the corneal epithelium. Acta Ophthalmol. Scand. 75, 383–387.
Robin, J.S., Ellis, P.P., 1978. Ophthalmic ointments. Surv. Ophthalmol. 22, 335–340.
Rolando, M., Zierhut, M., 2001. The ocular surface and tear film and their dysfunction in dry eye disease. Surv. Ophthalmol. 45 (Suppl. 2), S203–S210.
Sanitato, J.J., Asbell, P.A., Varnell, E.D., Kissling, G.E., Kaufman, H.E., 1984. Acyclovir in the treatment of herpetic stromal disease. Am. J. Ophthalmol. 98, 537–547.
Shah, V.P., Flynn, G.L., Yacobi, A., Maibach, H.I., Bon, C., Fleischer, N.M., Franz, T.J., Kaplan, S.A., Kawamoto, J., Lesko, L.J., Marty, J.P., Pershing, L.K., Schaefer, H., Sequeira, J.A., Shrivastava, S.P., Wilkin, J., Williams, R.L., 1998. Bioequivalence of topical dermatological dosage forms—methods of evaluation of bioequivalence. Pharm. Res. 15, 167–171.
Tabbara, K.F., Al Balushi, N., 2010. Topical ganciclovir in the treatment of acute herpetic keratitis. Clin. Ophthalmol. (Auckl., NZ) 4, 905–912.
USP38-NF33, 2015. General Chapter <1724> Semisolid Drug Products-Performance Tests. US Pharmacopeia, Rockville, MD, USA, 1625-1637 pp. Available at http://www.uspnf.com/uspnf/pdf/download?usp=36&nf=31&s=2&q=usp36nf31s2_c1724.pdf&officialOn=December (accessed 19.05.15.).
VanderWerf, F., Brassinga, P., Reits, D., Aramideh, M., Ongerboer de Visser, B., 2003. Eyelid Movements: Behavioral Studies of Blinking in Humans Under Different Stimulus Conditions. J Neurophysiol. 89 (May (5)), 2784–2796.
Wen, Q., Trokel, S.L., Paik, D.C., 2013. Aliphatic β-nitroalcohols for therapeutic corneoscleral cross-linking: corneal permeability considerations. Cornea 32, 179–184.
Werkmeister, R.M., Alex, A., Kaya, S., Unterhuber, A., Hofer, B., Riedl, J., Bronhagl, M., Vietauer, M., Schmidl, D., Schmoll, T., Garhöfer, G., Drexler, W., Leitgeb, R.A., Groeschl, M., Schmetterer, L., 2013. Measurement of tear film thickness using ultrahigh-resolution optical coherence tomography. Invest. Ophthalmol. Vis. Sci. 54, 5578–5583.
Wilhelmus, K.R., Hyndiuk, R.A., Caldwell, D.R., Abshire, R.L., Folkens, A.T., Godio, L.B., 1993. 0.3% ciprofloxacin ophthalmic ointment in the treatment of bacterial keratitis. Arch. Ophthalmol. Chic. 111, 1210–1218.
Wolff, E., 1946. The mucocutaneous junction of the lidmargin and the distribution of the tear fluid. Trans. Am. Ophthalmol. Soc. 66, 291–308.
Xu, X., Al-Ghabeish, M., Krishnaiah, Y.S.R., Rahman, Z., Khan, M., 2015. Kinetics of drug release from ointments: role of transient-boundary. Int. J. Pharm. doi: http://dx.doi.org/10.1016/j.ijpharm.2015.07.077.